Journal of Experimental Nanoscience

ISSN: 1745-8080 (Print) 1745-8099 (Online) Journal homepage: informahealthcare.com/journals/tjen20

# Comparative cytotoxicity evaluation of different size gold nanoparticles in human dermal fibroblasts

Diego Mateo, Paloma Morales, Alicia Ávalos & Ana I. Haza

**To cite this article:** Diego Mateo, Paloma Morales, Alicia Ávalos & Ana I. Haza (2015) Comparative cytotoxicity evaluation of different size gold nanoparticles in human dermal fibroblasts, Journal of Experimental Nanoscience, 10:18, 1401-1417, DOI: 10.1080/17458080.2015.1014934

**To link to this article:** https://doi.org/10.1080/17458080.2015.1014934

Published online: 27 Feb 2015.

*Journal of Experimental Nanoscience*, 2015
Vol. 10, No. 18, 1401–1417, http://dx.doi.org/10.1080/17458080.2015.1014934



# Comparative cytotoxicity evaluation of different size gold nanoparticles in human dermal fibroblasts

Diego Mateo, Paloma Morales, Alicia Ávalos and Ana I. Haza*

*Departamento de Nutrición, Bromatología y Tecnología de los Alimentos, Facultad de Veterinaria, Universidad Complutense de Madrid, 28040 Madrid, Spain*

(*Received 23 July 2014; final version received 30 January 2015*)

The aim of this work was to compare the effects of three commercially available gold nanoparticles (AuNPs) of different sizes (30, 50 and 90 nm) on the viability of normal human dermal fibroblasts (NHDF). In addition, we evaluated protective effect of *N*-Acetyl-L-cysteine (NAC), total glutathione content (GSH/GSSG), superoxide dismutase (SOD) activity and reactive oxygen species (ROS) production to investigate if oxidative stress was involved in the cytotoxic response of these AuNPs. Although AuNP-induced cytotoxicity was dose and time dependent, nanoparticle size slightly influenced the cytotoxic response of AuNPs assessed by 3-(4,5-dimethylthiazol-2-yl)-2,5-diphenyltetrazolium bromide and lactate dehydrogenase. Regarding oxidative parameters, NAC produced no significant protection of NHDF cells against treatment with any of the three AuNPs. Independently on nanoparticle size, GSH/GSSG content was drastically depleted after 24 h of incubation with the three AuNPs (less than 15% in all cases), while no statistically significant changes on SOD activity were reported (~90% of activity). The three AuNPs also caused a notable increase in the ROS production of NHDF cells. In conclusion, our data suggest that AuNP-induced cytotoxicity in NHDF is mediated by oxidative stress and it is independent of nanoparticle size.

**Keywords:** gold nanoparticles; dermal fibroblasts; cytotoxicity; oxidative stress

## 1. Introduction

Nanoparticles (NPs), defined as particles with at least one dimension in the size range of 1–100 nm, are being applied in production of exceptional devices at the nanoscale level due to their unique physical and chemical functional properties.[1] Their applications include multiple areas like medicine, engineering, manufacture and food industry, but also many consumer products such as food storage devices, health care products and cosmetics.[2–4]

The great increase in the human exposure to nanosized particles over the last years has awaken the interest in the potential environmental and health impact of nanomaterials.[5] NPs are believed to be more biologically reactive than their bulk counter-parts due to their small size and larger surface area to volume ratio.[6] As a consequence of this considerable biological activity, NPs may produce oxidative effects at the cellular level.[1] Moreover, NPs easily travel through the body, deposit in target organs, penetrate cell membranes and may trigger harmful responses such as alterations of calcium homeostasis and gene

*Corresponding author. Email: hanais@vet.ucm.es

expression, inflammation and DNA damage.[7–9] Despite this, to date there is a lack of regulated methods and safety guidelines to evaluate the risk associated with the exposure to nanomaterials.[10]

Current applications of metallic NPs cover a wide range of industrial and consumer sectors including cosmetics, medicine and material science.[11] Concretely, as a result of their optical, chemical and electronic properties, gold nanoparticles (AuNPs) are expected to be successfully employed in many biomedical applications such as drug/gene delivery, imaging and diagnostics.[12,13] Although gold has been traditionally considered inert and biocompatible, higher reactivity than that observed in the bulk material can arise at nanoscale.[14] Some studies have reported the potential cytotoxicity of AuNPs, which has been demonstrated to depend on their size, surface charge and shape.[15,16] The production of reactive oxygen species (ROS) leading to oxidative stress is considered as one of the responsible factor for nanomaterials toxicity, as several studies with AuNPs have demonstrated in HeLa, HepG2 (human hepatoma) and PMBC cells.[17–19] Therefore, the assessment of the health risks arising from the exposure to AuNPs has become a crucial issue.[20]

Dermal exposure is considered one of the most important uptake routes of NPs and it occurs regularly during the use of coated products or due to topical application of chemicals or drugs.[21,22] Some papers have suggested that NPs can be the promising candidates for transdermal drug delivery owing to their biocompatibility, low toxicity and small size.[23,24] In particular, the effect of AuNPs combined with anti-oxidants has shown a notable acceleration in diabetic wound healing.[25,26] AuNPs have also been extensively incorporated to many consumer products such as cosmetics, soaps and dressings as a result of their surprisingly strong anti-oxidant, anti-microbial and anti-inflammatory properties, which make them useful agents in the treatment against rheumatoid arthritis and topical wounds.[27–29] Furthermore, it has previously shown that AuNPs may be used in the future for the treatment of cutaneous infectious diseases or skin cancers.[30,31] Taken together, all these findings evidence that skin is one of the main potential portals of entry of AuNPs to human organism.

As we have mentioned before, NPs cytotoxicity has been evidenced to depend not only on their shape, surface chemistry or size, but also on the cell line studied. Former investigations from our group described AuNP-induced cytotoxicity on two tumour cell lines, HL-60 (human peripheral blood promyelocytic leukaemia cells) and HepG2.[32] The *in vitro* assessment of human fibroblast toxicity has been traditionally considered as an appropriate tool to describe cytotoxicity of topically applied substances.[33] Skin tissue, which represents the first barrier against exposure to environmental factors containing NPs, is mostly constituted by dermal fibroblasts.[34] In addition, in the wound healing process, dermal fibroblasts are the main cell types implicated in the extracellular matrix production.[35] Furthermore, current literature regarding cytotoxic responses of dermal fibroblast exposed to AuNPs is very limited. For these reasons, we chose normal human dermal fibroblast (NHDF) cells as a model in our study. Thus, the main objective of this paper was to compare the effects of commercially available AuNPs of similar shape but different sizes (30, 50 and 90 nm) on NHDF cells. Cytotoxicity was assessed by metabolic inhibition and loss of cellular membrane integrity. Moreover, we evaluated protective effect of *N*-Acetyl-L-cysteine (NAC), total glutathione content (GSH/GSSG), superoxide dismutase (SOD) activity and intracellular ROS production to characterise the potential of AuNPs to induce oxidative stress.

## 2. Methods

### 2.1. Chemicals

All chemicals were reagent grade or higher and were obtained from Sigma-Aldrich (St. Louis, MO, USA), unless otherwise specified. Water-based solutions of AuNPs of 30 (Cat. no. 08-79-6040), 50 (Cat. no. 08-79-6045) and 90 nm (Cat. no. 08-79-6055) in diameter were purchased from CymitQuímica (Barcelona, Spain). Stock solutions of AuNPs were diluted to the required concentrations using the respective cell culture medium. NAC was purchased from Sigma-Aldrich (St. Louis, MO, USA). 2′-7′-dichlorodihydrofluorescein diacetate ($H_2$DCFDA) was obtained from Molecular Probes (Eugene, OR, USA). Culture medium and supplements required for the growth of the NHDF cell line were purchased from PromoCell Gmbh (Heidelberg, Germany).

### 2.2. Cell culture

NHDF were obtained from PromoCell GmbH (Heidelberg, Germany). Only cells of passage 10–17 were used in the experiments. NHDF cells were cultured as monolayer in fibroblast basal medium supplemented with 2% v/v heat-inactivated fetal bovine serum (FBS), 1% v/v penicillin–streptomycin, 5 μg/mL insulin and 1 ng/mL basic fibroblast growth factor. All human cell cultures were incubated at 37 °C and 100% humidity in a 5% $CO_2$ atmosphere.

### 2.3 Characterisation of nanoparticles

Morphology and size distribution of AuNPs aqueous solutions were estimated by transmission electron microscopy (TEM) in a previous work.[32] In addition, AuNPs were observed after incubation in cell-free culture media (70% v/v) for 24 h at 37 °C to reach a representative number of AuNPs. Image J software was used to measure the size of NPs. The mean and standard deviation (SD) of particle sizes were calculated from measuring over 100 NPs in random fields of view in addition to the images showing the general morphology of the NPs, as previously described by Murdock et al.[36]

Furthermore, dynamic light scattering (DLS) was used for the characterisation of hydrodynamic size of AuNPs suspended for 24 h in cell-free culture medium performed on a Malvern Instruments Zetasizer Nano-ZS from National Institute of Agricultural and Food Research and Technology (INIA), Madrid, Spain as described by Murdock et al.[36] The method yields a hydrodynamic diameter, which is a calculated particle diameter of a sphere that has the same measured motion in the solute as the actual particle.

### 2.4. Cytotoxicity endpoints

#### 2.4.1. MTT assay

MTT (3-(4,5-dimethylthiazol-2-yl)-2,5-diphenyltetrazolium bromide) reduction and lactate dehydrogenase (LDH) leakage were used as parameters for cytotoxicity assessment. MTT is based on the mitochondrial reduction of tetrazolium salt (MTT) into an insoluble formazan product by succinate dehydrogenase. The assay was assessed according to the

manufacturer's instructions (Cell Proliferation Kit I, Roche, IN, USA). Briefly, NHDF cells ($5 \times 10^5$ cells/mL) were plated onto 96-multiwell systems and incubated in complete culture medium for 24 h to grow cells as monolayer, prior to the treatment with AuNPs. Subsequently, 100 μL of different concentrations of AuNPs (1−25 μg/mL) or negative controls (without AuNPs) were added to each well. Plates were then incubated for 24, 48 and 72 h at 37 °C and 100% humidity in a 5% $CO_2$ atmosphere. The optical density of each well was read at 620 nm (test wavelength) and 690 nm (reference wavelength) by an UV-Visible absorbance microplate reader with a built-in software package for data analysis (iEMS Reader MF, Labsystems, Helsinki, Finland).

Values presented in this paper are mean ± standard error of the mean (SEM). Results were expressed as the percentage of survival (%SDH) with respect to the control cells according to the following equation: % SDH activity = $(A_1/A_0) \times 100$, where $A_1$ is the absorbance of the cells exposed to the AuNPs, and $A_0$ is the absorbance of the negative control (cells without AuNPs). All NPs concentrations were tested in 16 replicates and the experiments were repeated three independent times.

#### *2.4.2. LDH assay*

Membrane integrity was assessed by measuring extracellular LDH using a commercially available kit [cytotoxicity detection kit (LDH), Roche Diagnostic, IN, USA]. Cytosolic LDH is released into the culture medium if the integrity of the cell membrane deteriorates in cells suffering from irreversible cell death. Briefly, NHDF cells were seeded in 96-well plates at a density of $5 \times 10^5$ cells/mL culture medium. After 24 h of seeding, 100 μL of different concentrations of AuNPs (1−25 μg/mL) or negative and positive controls were added to the wells. Plates were then incubated for different times 24, 48 and 72 h at 37 °C and 100% humidity in a 5% $CO_2$ atmosphere. Cell-free culture media was collected and incubated with the same volume of reaction mixture for 30 min. LDH activity was measured at 490 nm by an UV-Visible absorbance microplate reader with a built-in software package for data analysis (iEMS Reader MF, Labsystems, Helsinki, Finland). Background and negative controls were obtained by LDH measurement of assay medium and untreated cell medium, respectively. Total cellular LDH activity (positive control) was measured in cell lysates obtained by treatment with TritonX-100 solution.

The percentage of LDH leakage was calculated as follows: LDH leakage (%) = (experimental value − untreated control) / (positive control − untreated control) × 100 and represents the mean of three independent experiments, each using 12 wells per concentration.

Using data from MTT and LDH, the half inhibitory concentration ($IC_{50}$), which quantifies the concentration of each nanoparticle to inhibit cell growth by half after 24 h, was obtained.

### *2.5. Effect of NAC in AuNPs-derived cytotoxicity*

The protective effect of NAC, an important anti-oxidant precursor for the synthesis of glutathione, against AuNPs-induced cytotoxicity was evaluated using the MTT assay.[37] NAC (20 mM) was added to NHDF cells 1 h before the addition of AuNPs at $IC_{50}$ concentrations.[32] Then, the procedure was same as the MTT assay described above.

### *2.6. Total glutathione content*

The total glutathione content (GSH/GSSG) was measured using a commercial colorimetric assay kit, OxiSelect Total Glutathione (Cell Biolabs, Inc., San Diego, USA). Glutathione reductase reduces oxidised glutathione (GSSG) to reduced glutathione (GSH/GSSG) in the presence of NADPH. Subsequently, the chromogen reacts with the thiol group of GSH/GSSG to produce a coloured compound. The assay was assessed according to the manufacturer's instructions. Briefly, NHDF cells were treated for 24, 48 and 72 h with AuNPs (each one at its MTT $IC_{50}$). After treatment with AuNPs, cells were centrifuged and washed with cold 1X phosphate-buffered saline (PBS). Subsequently, the pellet was resuspended with 200–500 μL ice-cold 0.5% metaphosphoric acid, centrifuged again at 1200 rpm for 5 min at 4 °C and the supernatant was collected. Then, 25 μL 1X glutathione reductase and 25 μL 1X NADPH were added to each well to be tested. Finally, 100 μL of the sample and 50 μL 1X chromogen were added. After a brief mixture, the absorbance was measured immediately at 405 nm by an UV-Visible absorbance microplate reader with a built-in software package for data analysis (iEMS Reader MF, Labsystems, Helsinki, Finland), with two-minute reading intervals for 10 min. The total glutathione content was determined by comparison with the predetermined glutathione standard curve. Results were expressed as percentage of total glutathione content (GSH/GSSG).

### *2.7. Superoxide dismutase activity*

SOD activity was measured according to the method OxiSelect Superoxide Dismutase Activity (Cell Biolabs, Inc., San Diego, USA). Superoxide anions ($O_2^-$) are generated by xanthine/xanthine oxidase (XOD) system and detected with a chromogen solution. However, in presence of SOD the superoxide anion concentration is reduced. Briefly, NHDF cells were treated for 24, 48 and 72 h with AuNPs (each one at its MTT $IC_{50}$). After treatment, cells were washed with cold 1X PBS and incubated on ice with 1X lysis Buffer (10 mM Tris, pH 7.5, 150 mM NaCl, 0.1 mM EDTA, 0.5% Triton X-100) for 10 min. Following, cells were centrifuged at 12.000 × *g* for 10 min, and the cell lysate supernatant was collected. 10 μL of supernatant was added to each well to be tested. Finally, 80 μL of master mixture (containing xanthine solution, chromogen, lysis buffer and water) and 10 μL of prediluted 1X XOD solution were added and the absorbance was read immediately at 492 nm by an UV-Visible absorbance microplate reader with a built-in software package for data analysis (iEMS Reader MF, Labsystems, Helsinki, Finland).

The results were expressed as percentage of SOD activity (% activity) and were calculated as follows: SOD activity = $[(A_0 - A_1)/A_0] \times 100$, where $A_0$ is the absorbance of the negative control, and $A_1$ is the absorbance of the cells exposed to the AuNPs.

### *2.8. Measurement of intracellular ROS production*

ROS production was determined using $H_2$DCFDA. The principle of this assay is that $H_2$DCFDA diffuses through the cell membrane and is enzymatically hydrolysed by intracellular esterases to non-fluorescent dichlorohydrofluorescein (DCFH). In the presence of ROS, this compound is rapidly oxidised to highly fluorescent dichlorofluorescein (DCF). NHDF cells were treated with AuNPs (each one with its MTT $IC_{50}$) for different time intervals (15 min–48 h). Then, $3 \times 10^5$ cells were washed with PBS

loaded for 30 min with $H_2$DCFDA (10 μM) and incubated in a water bath (37 °C). The cells were kept on ice and the fluorescence intensity was read immediately with a FACS Calibur flow cytometer (Becton and Dickinson, Franklin Lakes, NJ, USA) and the CellQuest software from Cytometry and Fluorescence Microscopy Centre, Complutense University, Madrid, Spain. For each experiment, $10^4$ cells were analysed.

### *2.9. Statistical analysis*

Each experiment was performed at least three times. Results are expressed as mean ± SEM. Data were subjected to statistical analyses by the Student's *t*-test to determine significance ($p < 0.05$) relative to the unexposed control. All tests were performed with the software package StatgraphicsPlus 5.0.

## 3. Results

### *3.1 Characterisation of AuNPs*

Commercially produced 30, 50 and 90 nm AuNPs were examined by TEM and DLS to determine the particle shape and size distribution. According to the results obtained by TEM and DLS analysis in aqueous solution, the characterisation of the three AuNPs corresponded with the data reported by the manufacturer (Table 1). After 24 h of incubation in cell-free medium, AuNPs found to show larger size measurements (Figure 1: 1A, 2A and 3A). In this study, we obtained an increase of 8 nm in the size of 30 nm AuNPs, while 50 and 90 nm AuNPs augmented approximately 20 nm their size (Table 1). The DLS analysis of the AuNPs subsequent to the addition of cell-free medium with 2% FBS (Figure 1: 1B, 2B and 3B) indicated the presence of aggregates and consequently reported larger size distributions than those obtained in aqueous solution (Table 1).

### *3.2. Effect of AuNPs on cell viability*

The cytotoxicity of 30, 50 and 90 nm AuNPs was firstly investigated by measuring the cellular metabolic activity. The results of the MTT viability assay (Figure 2.1) showed that the three AuNPs were slightly cytotoxic toward the NHDF cells that were exposed at concentrations from 1 to 15 μg/mL and all incubation times (more than 65% of cell

Table 1. Size distribution of AuNPs measured by TEM and DLS.

| | Particle size (nm) | | |
|---|---|---|---|
| Measuring method | 30 | 50 | 90 |
| TEM (aqueous solution)[a] | 38.6 ± 6.1 | 56.1 ± 3.7 | 92.0 ± 6.2 |
| TEM in fibroblast medium 2% FBS | 46.3 ± 6.9 | 80.4 ± 5.9 | 115.5 ± 8.5 |
| DLS (aqueous solution)[a] | 46.7 ± 1.0 | 53.3 ± 0.5 | 90.6 ± 0.3 |
| DLS in fibroblast medium 2% FBS | 70.4 ± 0.5 | 96.3 ± 1.4 | 125.1 ± 1.0 |

[a] From Mateo et al.[32]
Data are reported as mean ± standard deviation (SD).

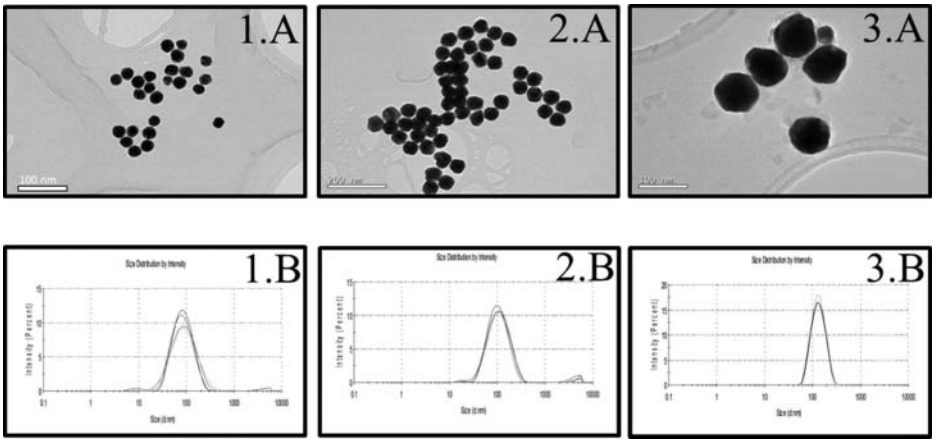


Figure 1. Analysis of 30 (1), 50 (2) and 90 (3) nm gold nanoparticles size by TEM and DLS. Representative TEM images (A) and size distribution by DLS (B) after 24 h incubation in cell-free culture medium. Scale bars represent 100 nm (1A and 3A) and 200 nm (2A).

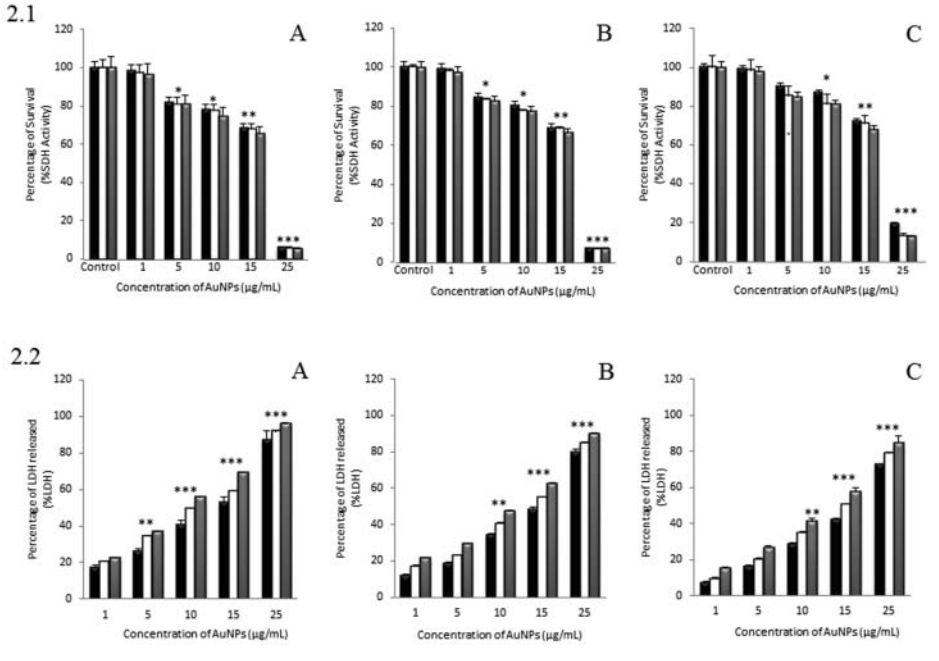


Figure 2. Effect of 30 nm (A), 50 nm (B) and 90 nm (C) AuNPs on NHDF cell viability by MTT (2.1) and LDH (2.2) assays. Cells were cultured with different concentrations of AuNPs for 24 (■), 48 (□) and 72 h (▒). Control, untreated cells. Asterisks indicate significant difference from control $^{***}$ $p \leq 0.001$, $^{**}$ $p \leq 0.01$ and $^{*}$ $p \leq 0.05$.

Table 2. Calculated $IC_{50}$ values in NHDF cell line determined by MTT and LDH.

| | $IC_{50}$ gold nanoparticles (μg/mL) | | | | | |
|---|---|---|---|---|---|---|
| Cell line | AuNP 30 nm | | AuNP 50 nm | | AuNP 90 nm | |
| | MTT | LDH | MTT | LDH | MTT | LDH |
| NHDF | 17.9 | 13.9 | 18.0 | 15.4 | 19.3 | 17.5 |

survival in all cases). However, cellular metabolic activity was almost completely reduced at the highest AuNPs dose assayed (25 μg/mL) and 72 h of treatment (5.1%, 7.1% and 13.0% of cell survival for 30, 50 and 90 nm AuNPs, respectively).

In addition to mitochondrial function, LDH leakage was measured as another indicator of AuNP-induced cytotoxicity (Figure 2.2). A significant LDH leakage, due to membrane damage, was determined after cells were treated with 30 nm AuNPs at 10 μg/mL for 72 h (55.8% of LDH leakage) (Figure 2(A)). In contrast, the treatment with 50 and 90 nm AuNPs (Figure 2.2(B) and 2.2(C)) under these same conditions did not reach a 50% of LDH leakage (47.7% and 41.4%, respectively). As it was observed in MTT assay, there was a significant LDH leakage after 72 h of treatment with the AuNPs at the highest concentration of 25 μg/mL studied (96.0%, 90.3% and 85.1% of LDH leakage for 30, 50 and 90 nm AuNPs, respectively).

The $IC_{50}$ values calculated from a regression curve are shown in Table 2. These values represent the effective concentration of AuNPs that decreases the amount of viable cells to 50% after 24 h. Values of $IC_{50}$ obtained by MTT assay resulted to be slightly higher than those obtained by LDH. Furthermore, comparison of the three different NPs in size showed that in NHDF cells 30 nm AuNPs resulted more cytotoxic in terms of metabolic activity and membrane integrity than 50 and 90 nm AuNPs.

### *3.3. Protective effect of* N-*Acetyl-L-cysteine (NAC)*

We measured the effect of pretreatment of NHDF cells with 20 mM NAC for 1 h prior to 24 h of incubation with the $IC_{50}$ of the three AuNPs (17.9, 18.0 and 19.3 μg/mL for 30, 50 and 90 nm AuNPs, respectively) (Figure 3). The pretreatment of NHDF cells with NAC

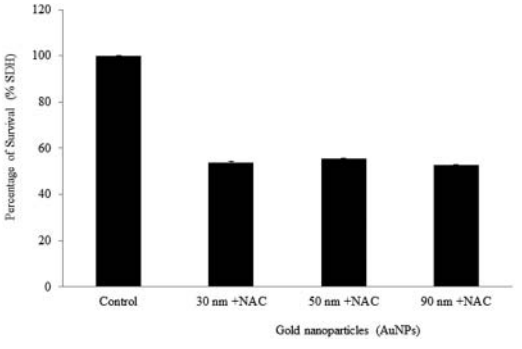


Figure 3. Effect of NAC on NHDF cell viability after the treatment with AuNPs. Cells were treated with $IC_{50}$ for 24 h. Control, untreated cells.

exhibited no significant protective effect towards any of the three different AuNPs in size, so the percentage of cell viability increased about 3.5%, 5.5% and 2.7% against the treatment with 30, 50 and 90 nm AuNPs, respectively.

### *3.4. Effect of AuNPs on total glutathione (GSH/GSSG) content*

A significant reduction of total glutathione content (GSH/GSSG) was reported after the treatment of NHDF cells with the three AuNPs at the $IC_{50}$ (17.9, 18.0 and 19.3 μg/mL for 30, 50 and 90 nm AuNPs, respectively) for 24, 48 and 72 h (Figure 4). GSH/GSSG levels relative to control were depleted to 7.8%, 13.1% and 11.8% after 24 h of treatment with 30, 50 and 90 nm AuNPs, respectively. Total gluthatione content decreased almost completely after 48–72 h of incubation with the three AuNPs (less than 2% of GSH/GSSG), noticing no difference among the three different sizes.

### *3.5. Effect of AuNPs on SOD activity*

The effect of AuNPs treatment on SOD activity in NHDF cells is shown in Figure 5. NHDF cells treated with the three AuNPs at the $IC_{50}$ (17.9, 18.0 and 19.3 μg/mL for 30, 50 and 90 nm, respectively) exhibited statistically insignificant changes in the SOD activity with respect to control group, independently on the incubation time and nanoparticle size.

### *3.6. Effect of AuNPs on ROS production*

The production of ROS in NHDF cell line after 0.25–48 h of treatment with the $IC_{50}$ of 30, 50 and 90 nm AuNPs (17.9, 18.0 and 19.3 μg/mL, respectively) is shown in Figure 6. DCF fluorescence was measured by flow cytometry and expressed as a percentage of control. The maximum production of ROS was determined after the treatment with 50 nm AuNPs.

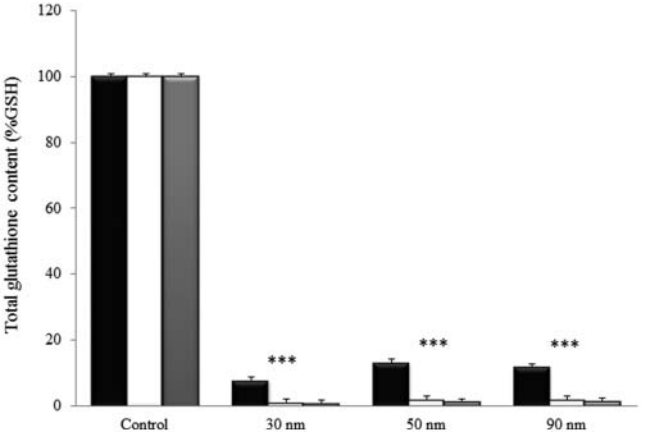


Figure 4. Effect of AuNPs on the total glutathione content in NHDF cells. Cells were treated with the $IC_{50}$ for 24 (■), 48 (□) and 72 h (▒). Control, untreated cells. Asterisks indicate significant difference from control $^{***}$ $p \leq 0.001$.

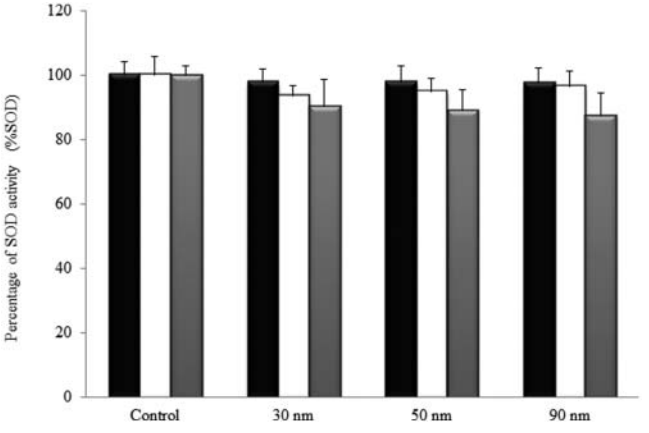


Figure 5. Effect of AuNPs on the SOD activity in NHDF cells. Cells were treated with the $IC_{50}$ for 24 (■), 48 (□) and 72 h (▒). Control, untreated cells.

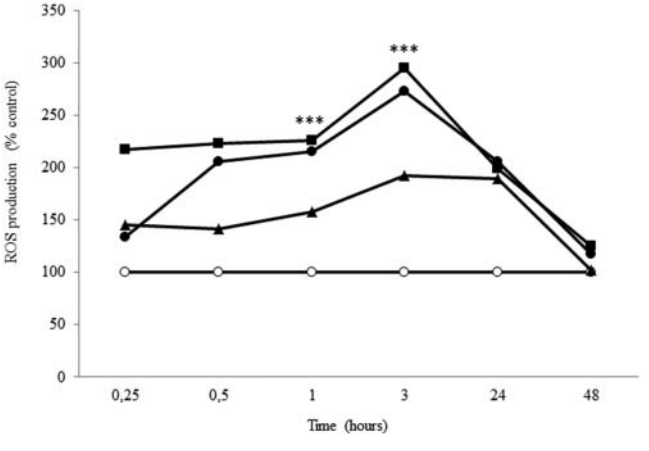


Figure 6. Time course of ROS production in NHDF cells, untreated (○) and treated with the $IC_{50}$ AuNPs of 30 nm (●), 50 nm (■) and 90 nm (▲). Asterisks indicate significant difference from control $^{***}$ $p \leq 0.001$.

ROS production began immediately after exposure of NHDF cells to the AuNPs, with a significant production after 1 h of incubation. However, it reached its maximum level after 3 h of treatment with AuNPs of 30 nm (2.73-fold), 50 nm (2.95-fold) and 90 nm (1.93-fold) at the $IC_{50}$. The production of ROS decreased gradually and it was reduced to nearly the basal level after 48 h.

## 4. Discussion

Despite the advantages of nanotechnology and the widespread use of products containing nanomaterials, studies indicate that NPs may cause hazardous effects due to their unique

physicochemical properties. The inherent beneficial effects of AuNPs have awaken notable interest in the treatment of topical wounds and skin pathologies such as rheumatoid arthritis, but potential cytotoxic responses of AuNPs should be considered when these products come into direct contact with skin, as it is the largest organ of the body and an important route of entry for NPs into the human organism.[22,29,38] Furthermore, since particle size is considered as a crucial factor when describing AuNP-induced cytotoxicity, in this study we evaluated the cytotoxic effects produced by three different AuNPs in size on NHDF cells and the role of oxidative stress in the observed cytotoxicity.

The size measurements of AuNPs in aqueous solution obtained by TEM and DLS were reported in a previous work of our group and validated the characteristics provided by the manufacturer (Table 1). In this study, data from TEM and DLS suggested that the cell culture medium containing 2% FBS affected the NPs dispersion (Figure 1). The high ionic strength of the medium reduces repulsive forces among the NPs, inducing aggregation, as other authors have observed.[39] These results can also be explained by the possible interaction of AuNPs with the cell culture media, which has been widely reported with different NPs that leads to the formation of 'protein corona'.[40] DLS measurements reported higher diameter profiles than those obtained by TEM (Table 1), but this differences are attributable to the different experimental conditions of both techniques.[41] Taken together, our results indicate that the fibroblast basal culture medium supplemented with 2% FBS caused nanoparticle aggregation. RPMI 1640 and Dulbecco's modified Eagle's culture media containing FBS have also proved to induce the aggregation of AuNPs.[32]

Currently there is a great controversy about AuNPs cytotoxicity, and it comes from the variability of parameters including cell lines used in toxicity assays, concentrations and coatings. According to MTT and LDH assays, the exposure of NHDF cells to the three different AuNPs in size produced a reduction in cell mitochondrial activity and a LDH leakage in a dose- and time-dependent manner (Figure 2.1 and 2.2). A study by Mironava et al. [42] also showed that AuNPs could penetrate the plasma membrane and cause cell damage to human dermal fibroblast. However, data are still so far inconclusive, as several studies have demonstrated that the treatment of human dermal fibroblasts with AuNPs affects cell morphology but not cell viability.[43,44] Thus, further studies would be needed to clarify this point.

In addition, results from this work showed that AuNP-induced cytotoxicity was slightly dependent on nanoparticle size, as we described in a preceding study with HL-60 and HepG2 tumour cells.[32] The cytotoxic effects were somewhat stronger after the treatment of cells with 30 nm AuNPs than those obtained with the 50 and 90 nm NPs-treated cells (Table 2). Thus, we reported very short differences between the cytotoxic response of three NPs studied, despite the size is considered as a decisive factor when describing cytotoxicity, tissue distribution and cell absorption of silver and AuNPs.[5] The cytotoxic response of several cell lines exposed to AuNPs of 1 and 15 nm in diameter was studied by Pan et al. [15] and it was demonstrated that after 48 h of treatment, smaller AuNPs had a wider distribution and a higher toxic potential than larger ones. Coradeghini et al. [45] described the interactions of 5 and 15 nm AuNPs with mouse fibroblasts and found that 5 nm AuNPs were responsible of major cell damage. Other metallic NPs have shown similar size-dependent cytotoxicity behaviour. A comparative study with silver NPs of 4.7 and 42 nm determined that small NPs were much more cytotoxic to cells than large ones.[46] Accordingly, Xiong et al. [47] observed a major

cytotoxic response in cells treated with 10 nm $TiO_2$ NPs than those treated with larger NPs of 20 and 100 nm in size.

Former investigations have found different cell responses to metallic NPs cytotoxicity depending on the cell line studied. In a study by Choi et al. [48] AuNPs of 17 nm in diameter exhibited different cytotoxic effects on human lung carcinoma cells (A549 and NCI-H1975) and human epidermoid cells (A431), resulting in $IC_{50}$ values of 48.9, 52.3 and 65.2 μg/mL, respectively. Uboldi et al. [49] reported different cell responses to AuNPs when they observed no effect on the viability of human alveolar type-II cell line NCI441 while A549 cells exhibited a moderate cytotoxicity under the exposure with AuNPs. Moreover, other study reported $IC_{50}$ values of 838 and 1028 μg/mL on prostate and breast cancer cells treated with spherical AuNPs of 1.9 nm, respectively.[50]

To clarify if oxidative stress was involved in AuNP-induced cytotoxicity, we studied the protective effect of anti-oxidant NAC. Under our experimental conditions, NHDF cells pretreated with NAC did not report any significant protection against 30, 50 and 90 nm AuNPs cytotoxicity (Figure 3). In contrast to our results, Zhao et al. [51] suggested that the detoxification mechanism of NAC could consist on its effective binding through thiol groups to AuNPs, which would avoid the generation of ROS. Surprisingly, a previous work from our group described this protective effect of NAC against 30, 50 and 90 nm cytotoxic effect on HL-60 and HepG2, so these discoveries suggest a possible cell-type dependent protective response of NAC.[32]

Glutathione is considered the most abundant thiol in cells and determines the intracellular redox potential.[52] Total GSH/GSSG content was significantly depleted after treatment of human dermal fibroblasts with the three AuNPs of different sizes (Figure 4). In the literature, many studies have reported a comparable behaviour on cells exposed to metallic nanomaterials such as copper, titanium, silver and gold.[53–56] These findings, together with our results, demonstrate that the interaction between GSH/GSSG and AuNPs represents an important detoxification mechanism towards cytotoxicity induced by AuNPs, as other authors have formerly suggested.[57]

In contrast to the results of total GSH/GSSG content, human dermal fibroblasts exposed to the three AuNPs of 30, 50 and 90 nm exhibited no statistically significant changes in the activity of SOD (Figure 5). Previous works have reported different responses of cellular defence mechanisms to oxidative stress induced by silver NPs.[58] Taken together, results from protective effect of NAC, total GSH/GSSG content and SOD activity suggest that these protection mechanisms could be determined by the cell line studied.

Metallic NPs are considered as a primary source of ROS, which represent an important mechanism of oxidative stress in cells.[59,60] Here we observed a significant ROS production, which indicates that one of the primary mechanisms of AuNP-induced cytotoxicity in NHDF cells might be oxidative stress (Figure 6). Data from literature regarding ROS production of AuNPs are somehow conflicting. Aueviriyavit et al. [55] reported no change in the ROS intracellular levels of Caco-2 cells treated with AuNPs. On the other hand, some authors have demonstrated the involvement of ROS production and oxidative stress in AuNP-induced toxicity *in vitro* and *in vivo*.[61–63] Furthermore, in this study maximum ROS levels were obtained after the treatment with 50 nm AuNPs. These findings demonstrate that nanoparticle size could play an important role in the ROS production by AuNPs. Thus, ROS production induced by AuNPs might be cell-type specific or might be determined by the different parameters of each study, including particle size or coating.

In conclusion, our results indicate that the exposure of NHDF cells to AuNPs affected negatively cellular metabolic activity and membrane stability, independently on nanoparticle size. Depletion of total glutathione content and ROS production suggests that oxidative stress contributes to AuNPs-induced cytotoxicity, which appears to be somehow determined by cell line. Thus, in comparison with our previous study with HL-60 and HepG2 tumour cells, human dermal fibroblasts have proved to be more sensible to total glutathione depletion and ROS production after exposure with AuNPs. In view of these findings, AuNPs should be used carefully for the topical treatment of wounds or other skin pathologies owing to their potential hazardous behaviour. In addition, regulatory agencies should develop safety guidelines and take into account risk assessment of these AuNPs to avoid negative effects on consumers. Further studies in our group are encouraged to clarify if exposure to these AuNPs could induce apoptosis or genotoxic events, as it has been previously described.[61–64].

## Disclosure statement

The authors report that there was no conflict of interest in this study.

## Funding

This work was supported by Ministerio de Educación, Cultura y Deporte (Spain) [grant number AGL2010-16561]; A. Ávalos is a recipient of a fellowship from the Ministerio de Educación, Cultura y Deporte (Spain).

## References

[1] Oberdorster G, Maynard A, Donaldson K, Castranova V, Fitzpatrick J, Ausman K, Carter J, Karn B, Kreyling W, Lai D, Olin S, Monteiro-Riviere N, Warheit D, Yang H, ILSI Research Foundation/Risk Science Institute Nanomaterial Toxicity Screening Working Group. Principles for characterizing the potential human health effects from exposure to nanomaterials: elements of a screening strategy. Part Fibre Toxicol. 2005;2:8.

[2] Silvestre C, Duraccio D, Cimmino S. Food packaging based on polymer nanomaterials. Prog Polymer Sci. 2011;36:1766–1782.

[3] Wise JP, Goodale BC, Wise SS, Craig GA, Pongan AF, Walter RB, Thompson WD, Ng AK, Aboueissa AM, Mitani H, Spalding MJ, Mason MD. Silver nanospheres are cytotoxic and genotoxic to fish cells. Aquatic Toxicol. 2010;97:34–41.

[4] Farkas J, Christian P, Urrea JA, Roos N, Hassellov M, Tollefsen KE, Thomas KV. Effects of silver and gold nanoparticles on rainbow trout (*Oncorhynchus mykiss*) hepatocytes. Aquatic Toxicol. 2010;96:44–52.

[5] Johnston HJ, Hutchison G, Christensen FM, Peters S, Hankin S, Stone V. A review of the *in vivo* and *in vitro* toxicity of silver and gold particulates: particle attributes and biological mechanisms responsible for the observed toxicity. Crit Rev Toxicol. 2010;40:328–346.

[6] Lanone S, Boczkowski J. Biomedical applications and potential health risks of nanomaterials: molecular mechanisms. Curr Mol Med. 2006;6:651–663.

[7] Roy R, Kumar S, Tripathi A, Das M, Dwivedi PD. Interactive threats of nanoparticles to the biological system. Immunol Lett. 2014;158:79–87.

[8] Deng ZJ, Liang M, Monteiro M, Toth I, Minchin RF. Nanoparticle-induced unfolding of fibrinogen promotes Mac-1 receptor activation and inflammation. Nat Nanotechnol. 2011;6:39–44.

[9] Bhabra G, Sood A, Fisher B, Cartwright L, Saunders M, Evans WH, Surprenant A, Lopez-Castejon G, Mann S, Davis SA. Nanoparticles can cause DNA damage across a cellular barrier. Nat Nanotechnol. 2009;4:876–883.
[10] Chuang SM, Lee YH, Liang RY, Roam GD, Zeng ZM, Tu HF, Wang SK, Chueh PJ. Extensive evaluations of the cytotoxic effects of gold nanoparticles. Biochimica Biophysica Acta. 2013;1830:4960–4973.
[11] Som C, Wick P, Krug H, Nowack B. Environmental and health effects of nanomaterials in nanotextiles and Façade coatings. Environ Int. 2011;37:1131–1142.
[12] Lim ZZ, Li JE, Ng CT, Yung LY, Bay BH. Gold nanoparticles in cancer therapy. Acta Pharmacologia Sinica. 2011;32:983–990.
[13] Sperling RA, Gil Pra, Zhang F, Zanella M, Parak WJ. Biological applications of gold nanoparticles. Chem Soc Rev. 2008;37:1896–1908.
[14] Christian P, Von der Kammer F, Baalousha M, Hofmann T. Nanoparticles: structure, properties, preparation and behaviour in environmental media. Ecotoxicology. 2008;17:326–343.
[15] Pan Y, Neuss S, Leifert A, Fischler M, Wen F, Simon U, Schmid G, Brandau W, Jahnen-Dechent W. Size-dependent cytotoxicity of gold nanoparticles. Small. 2007;3:1941–1949.
[16] Arvizo RR, Miranda OR, Thompson MA, Pabelick CM, Bhattacharya R, Robertson JD, Rotello VM, Prakash YS, Mukherjee P. Effect of nanoparticle surface charge at the plasma membrane and beyond. Nano Lett. 2010;10:2543–2548.
[17] De Stefano D, Carnuccio R, Maiuri MC. Nanomaterials toxicity and cell death modalities. J Drug Deliv. 2012;2012:167896.
[18] Pan Y, Leifert A, Ruau D, Neuss S, Bornemann J, Schmid G, Brandau W, Simon U, Jahnen-Dechent W. Gold nanoparticles of diameter 1.4 nm trigger necrosis by oxidative stress and mitochondrial damage. Small. 2009;5:2067–2076.
[19] Paino IMM, Marangoni VS, de Oliveira Rita de Cássia S, Antunes LMG, Zucolotto V. Cyto and genotoxicity of gold nanoparticles in human hepatocellular carcinoma and peripheral blood mononuclear cells. Toxicol Lett. 2012;215:119–125.
[20] Fraga S, Faria H, Soares ME, Duarte JA, Soares L, Pereira E, Costa-Pereira C, Teixeira JP, de Lourdes Bastos M, Carmo H. Influence of the surface coating on the cytotoxicity, genotoxicity and uptake of gold nanoparticles in human HepG2 cells. J Appl Toxicol. 2013;33:1111–1119.
[21] Oberdorster G, Oberdorster E, Oberdorster J. Nanotoxicology: an emerging discipline evolving from studies of ultrafine particles. Environ Health Perspect. 2005;113:823–839.
[22] Park Y, Jeong SH, Yi SM, Choi BH, Kim Y, Kim I, Kim M, Son SW. Analysis for the potential of polystyrene and TiO2 nanoparticles to induce skin irritation, phototoxicity, and sensitization. Toxicol In Vitr. 2011;25:1863–1869.
[23] You CC, De M, Han G, Rotello VM. Tunable inhibition and denaturation of alpha-chymotrypsin with amino acid-functionalized gold nanoparticles. J Am Chem Soc. 2005;127:12873–12881.
[24] Pankhurst QA, Connolly J, Jones SK, Dobson J. Applications of magnetic nanoparticles in biomedicine. J Phys D. 2003;36:R167–R181.
[25] Chen S, Chen H, Yao Y, Hung C, Tu C, Liang Y. Topical treatment with anti-oxidants and au nanoparticles promote healing of diabetic wound through receptor for advance glycation end-products. Eur J Pharm Sci. 2012;47:875–883.
[26] Leu J, Chen S, Chen H, Wu W, Hung C, Yao Y, Tu C, Liang Y. The effects of gold nanoparticles in wound healing with antioxidant Epigallocatechin Gallate and $\alpha$-Lipoic acid. Nanomed Nanotechnol. 2012;8:767–775.
[27] Arockiya Aarthi Rajathi F, Arumugam R, Saravanan S, Anantharaman P. Phytofabrication of gold nanoparticles assisted by leaves of *Suaeda monoica* and its free radical scavenging property. J Photochem Photobiol B. 2014;135:75–80.

[28] Lokina S, Suresh R, Giribabu K, Stephen A, Lakshmi Sundaram R, Narayanan V. Spectroscopic investigations, antimicrobial, and cytotoxic activity of green synthesized gold nanoparticles. Spectrochimica Acta A. 2014;129:484–490.
[29] Unrau KR, Cavanagh MH, Cheng OK, Wang S, Burrell RE. Incorporating gold into nanocrystalline silver dressings reduces grain boundary size and maintains suitable antimicrobial properties. Int Wound J. 2013;10:666–674.
[30] Green HN, Martyshkin DV, Rodenburg CM, Rosenthal EL, Mirov SB. Gold nanorod bioconjugates for active tumor targeting and photothermal therapy. J Nanotech. 2011. doi:10.1155/2011/631753
[31] Mohebali M, Shahverdi AR, Rezayat SM, Edrissian GH, Esmaeili JSC, Charehdar S. Nanogold for the treatment of zoonotic cutaneous leishmaniasis caused by Leishmania major (MRHO/IR/75/ER): an animal trial with methanol extract of *Eucalyptus camaldulensis*. J Pharm Health Sci. 2012;1:13–16.
[32] Mateo D, Morales P, Ávalos A, Haza AI. Oxidative stress contributes to gold nanoparticle-induced cytotoxicity in human tumor cells. Toxicol Mech Methods. 2014;24:161–172.
[33] Hidalgo E, Bartolome R, Barroso C, Moreno A, Dominguez C. Silver nitrate: antimicrobial activity related to cytotoxicity in cultured human fibroblasts. Skin Pharmacol Appl Skin Physiol. 1998;11:140–151.
[34] Meyer K, Rajanahalli P, Ahamed M, Rowe JJ, Hong Y. ZnO nanoparticles induce apoptosis in human dermal fibroblasts via p53 and p38 pathways. Toxicol In Vitr. 2011;25:1721–1726.
[35] Hunt TK, Hopf HW. Wound healing and wound infection: what surgeons and anesthesiologists can do. Surg Clin North Am. 1997;77:587–606.
[36] Murdock RC, Braydich-Stolle L, Schrand AM, Schlager JJ, Hussain SM. Characterization of nanomaterial dispersion in solution prior to *in vitro* exposure using dynamic light scattering technique. Toxicol Sci. 2008;101:239–253.
[37] Ortolani O, Conti A, De Gaudio AR, Moraldi E, Cantini Q, Novelli G. The effect of glutathione and *N*-acetylcysteine on lipoperoxidative damage in patients with early septic shock. Am J Respir Crit Care Med. 2000;161:1907–1911.
[38] Messori L, Marcon G. Gold complexes in the treatment of rheumatoid arthritis. Chapter 9. In: Sigel A, Sigel H, editors. Ions in biological systems. Vol. 41. Cleveland, OH: CRC Press; 2004. p. 279–304.
[39] Fatisson J, Quevedo IR, Wilkinson KJ, Tufenkji N. Physicochemical characterization of engineered nanoparticles under physiological conditions: effect of culture media components and particle surface coating. Colloids Surface B Biointerfaces. 2012;91:198–204.
[40] Lundqvist M, Stigler J, Elia G, Lynch I, Cerdevall T, Dawson K. Nanoparticle size and surface properties determine the protein corona with possible implications for biological impacts. Proc Natl Acad Sci USA. 2008;105:14265–14270.
[41] Ito T, Sun L, Bevan MA, Crooks RM. Comparison of nanoparticle size and electrophoretic mobility measurements using a carbon-nanotube-based coulter counter, dynamic light scattering, transmission electron microscopy, and phase analysis light scattering. Langmuir. 2004;20:6940–6945.
[42] Mironava T, Hadjiargyrou M, Simon M, Jurukovski V, Rafailovich MH. Gold nanoparticles cellular toxicity and recovery: effect of size, concentration and exposure time. Nanotoxicology. 2010;4:120–137.
[43] Pernodet N, Fang X, Sun Y, Bakhtina A, Ramakrishnan A, Sokolov J, Ulman A, Rafailovich M. Adverse effects of citrate/gold nanoparticles on human dermal fibroblasts. Small. 2006;2:766–773.
[44] Qu Y, Lü X. Aqueous synthesis of gold nanoparticles and their cytotoxicity in human dermal fibroblasts-fetal. Biomed Mater. 2009;4:025007.

[45] Coradeghini R, Gioria S, García CP, Nativo P, Franchini F, Gilliland D, Ponti J, Rossi F. Size-dependent toxicity and cell interaction mechanisms of gold nanoparticles on mouse fibroblasts. Toxicol Lett. 2013;217:205–216.
[46] Avalos A, Haza AI, Mateo D, Morales P. Cytotoxicity and ROS production of manufactured silver nanoparticles of different sizes in hepatoma and leukemia cells. J Appl Toxicol. 2014;34:413–423.
[47] Xiong S, George S, Yu H, Damoiseaux R, France B, Ng K, Loo J. Size influences the cytotoxicity of poly (lactic-co-glycolic acid) (PLGA) and titanium dioxide (TiO2) nanoparticles. Arch Toxicol. 2013;87:1075–1086.
[48] Choi SY, Jeong S, Jang SH, Park J, Park JH, Ock KS, Lee SY, Joo SW. *In vitro* toxicity of serum protein-adsorbed citrate-reduced gold nanoparticles in human lung adenocarcinoma cells. Toxicol In Vitr. 2012;26:229–237.
[49] Uboldi C, Bonacchi D, Lorenzi G, Hermanns MI, Pohl C, Baldi G, Unger RE, Kirkpatrick CJ. Gold nanoparticles induce cytotoxicity in the alveolar type-II cell lines A549 and NCIH441. Part Fibre Toxicol. 2009;6:18-8977-6-18.
[50] Coulter JA, Jain S, Butterworth KT, Taggart LE, Dickson GR, McMahon SJ, Hyland WB, Muir MF, Trainor C, Hounsell AR, O'Sullivan JM, Schettino G, Currell FJ, Hirst DG, Prise KM. Cell type-dependent uptake, localization, and cytotoxicity of 1.9 nm gold nanoparticles. Int J Nanomed. 2012;7:2673–2685.
[51] Zhao Y, Gu X, Ma H, He X, Liu M, Ding Y. Association of glutathione level and cytotoxicity of gold nanoparticles in lung cancer cells. J Phys Chem C. 2011;115:12797–12802.
[52] Han G, Ghosh P, Rotello VM. Multi-functional gold nanoparticles for drug delivery. Adv Exp Med Biol. 2007;620:48–56.
[53] Alarifi S, Ali D, Verma A, Alakhtani S, Ali BA. Cytotoxicity and genotoxicity of copper oxide nanoparticles in human skin keratinocytes cells. Int J Toxicol. 2013;32:296–307.
[54] Botelho MC, Costa C, Silva S, Costa S, Dhawan A, Oliveira PA, Teixeira JP. Effects of titanium dioxide nanoparticles in human gastric epithelial cells *in vitro*. Biomed Pharmacother. 2014;58:59–64.
[55] Aueviriyavit S, Phummiratch D, Maniratanachote R. Mechanistic study on the biological effects of silver and gold nanoparticles in caco-2 cells – induction of the Nrf2/HO-1 pathway by high concentrations of silver nanoparticles. Toxicol Lett. 2014;224:73–83.
[56] Tournebize J, Boudier A, Joubert O, Eidi H, Bartosz G, Maincent P, Leroy P, Sapin-Minet A. Impact of gold nanoparticle coating on redox homeostasis. Int J Pharmaceutics. 2012;438:107–116.
[57] Gao W, Xu K, Ji L, Tang B. Effect of gold nanoparticles on glutathione depletion-induced hydrogen peroxide generation and apoptosis in HL7702 cells. Toxicol Lett. 2011;205:86–95.
[58] Arora S, Jain J, Rajwade JM, Paknikar KM. Cellular responses induced by silver nanoparticles: *in vitro* studies. Toxicol Lett. 2008;179:93–100.
[59] Kovacic P, Somanathan R. Biomechanisms of nanoparticles (toxicants, antioxidants and therapeutics): electron transfer and reactive oxygen species. J Nanosci Nanotechnol. 2010;10:7919–7930.
[60] Circu ML, Aw TY. Intestinal redox biology and oxidative stress. Semin Cell Dev Biol. 2012;23:729–737.
[61] Paino IMM, Marangoni VS, de Oliveira RCS, Antunes LMG, Zucolotto V. Cyto and genotoxicity of gold nanoparticles in human hepatocellular carcinoma and peripheral blood mononuclear cells. Toxicol Lett. 2012;215:119–125.
[62] Girgis E, Khalil WK, Emam AN, Mohamed MB, Rao KV. Nanotoxicity of gold and gold-cobalt nanoalloy. Chem Res Toxicol. 2012;25:1086–1098.

[63] Siddiqi NJ, Abdelhalim MA, El-Ansary AK, Alhomida AS, Ong WY. Identification of potential biomarkers of gold nanoparticle toxicity in rat brains. J Neuroinflamm. 2012;9:123. doi:10.1186/1742-2094-9-123

[64] Lan MY, Hsu YB, Hsu CH, Ho CY, Lin JC, Lee SW. Induction of apoptosis by high-dose gold nanoparticles in nasopharyngeal carcinoma cells. Auris Nasus Larynx. 2013;40:563–568.